The Korean Journal of Ceramics, **3** [3] 199 - 207 (1997)

Effects of the SiC Particle Size and Content on the Sintering and Mechanical Behaviors of Al_2O_3/SiC Particulate Composites

Jung-Ho Ryu and Jae-Hyung Lee

School of Metallurgical and Materials Engineering, Yeungnam University, Kyongsan-si, Kyongbuk, 712-749, Korea

(Received June 20, 1997)

Al_2O_3/SiC particulate composites were fabricated by pressureless sintering. The dispersed second phase was SiC of which the content was varied from 1.0 to 10 vol%. Three SiC powders having different median diameters from 0.28 μm to 1.9 μm were used. The microstructure became finer and more uniform as the SiC content increased except the 10 vol% specimens, which were sintered at a higher temperature. Under the same sintering condition, densification as well as grain growth was retarded more severely when the SiC content was higher or the SiC particle size was smaller. The highest flexural strength obtained at 5.0 vol% SiC regardless of the SiC particle size seemed to be owing to the finer and more uniform microstructures of the specimens. Annealing of the specimens at 1300°C improved the strength in general and this annealing effect was good for the specimens containing as low as 1.0 vol% of SiC. Fracture toughness did not change appreciably with the SiC content but, for the composites containing 10 vol% SiC, a significantly higher toughness was obtained with the specimen containing 1.9 μm SiC particles.

Key words : Particulate Composites, Nanocomposites, Alumina, SiC, Sintering, Mechanical Properties, Strength, Toughness, Crack Bridging

I. Introduction

Particulate composites containing fine second phase particles have been investigated widely in 1990's.[1-6] These so-called 'nanocomposites" have been controversial in terms of their potentially superior mechanical properties over those of monolithic ceramics. Niihara *et al.* first reported excellent mechanical properties for Al_2O_3 as well as Si_3N_4 reinforced with fine SiC particles.[1] They attributed the property improvement to crack deflection or microcracking around fine SiC particles. However, some other investigators' work, especially Zhao *et al.*,[7] found that SiC particles did not increase either intrinsic strength or toughness of Al_2O_3, but increased the strength only after a heat treatment. A similar controversy exists for Si_3N_4/SiC nanocomposites.[5] A few researchers still reviewed theoretically the possible mechanisms for property improvement in Al_2O_3/SiC nanocomposites.[3,4,9] One of the suggested mechanisms was that SiC particles inside the grain of Al_2O_3 but near the grain boundary gave compressive stresses to the grain boundary, which might strengthen the grain boundary and increase fracture toughness of the composite.[9] In this case, the strengthening effect was predicted to be the maximum at 5 vol% of fine SiC particles.

In this study, the amount of SiC particles was varied from 1 to 10 vol%. The SiC particle size was also varied from 0.28 μm to 1.9 μm to investigate the effect of the SiC particle size on the sintering behaviors, microstructures and mechanical properties of these particulate composites. In the particulate composites, fine particles tend to be trapped inside the matrix grains and large particles stay at the grain boundary. The location of the SiC particles in the composite may be important for the resultant mechanical properties. This study on the effect of the amount of particles as well as of the particle size on the mechanical properties may give hints to the possible strengthening mechanisms.

II. Experimental

The alumina powder used in this study was 99.995% pure α-Al_2O_3 of a 0.2 μm average particle size (Grade TM-DR, Taimei Chemicals Co. Ltd., Japan). Three different SiC powders were used; a fine α-SiC powder (Grade MSC-20, Mitsui Toatsu Chemicals, Inc., Japan, termed SiC powder F), medium-sized α-SiC (Grade A20, Hermann C. Starck, termed SiC powder M) and coarse α-SiC (Grade A10, Hermann C. Starck, termed SiC powder C). The particle size distribution of the SiC powders were determined using a light scattering method (Model SA-CP3, Shimadzu Co., Japan) and presented in Fig. 1. The SiC powder F had a relatively narrow particle size distribution with a median diameter (d_{50}) of 0.28 μm. On the other hand, powders M and C had wide particle size distributions with median diameters of 0.44 and 1.9 μm, respectively. In Fig. 2, the scanning electron micrographs of the three starting SiC powders are shown.

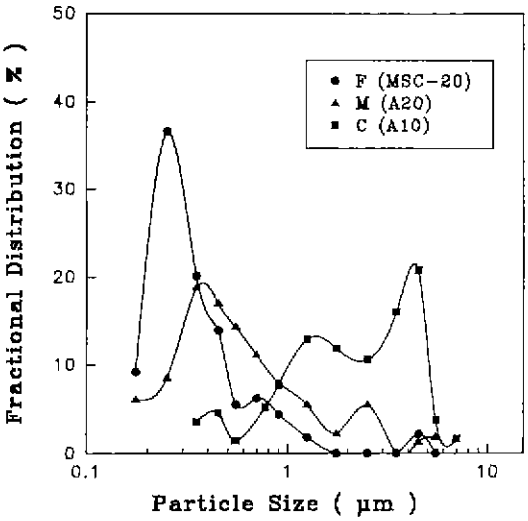

Fig. 1. Particle size distribution of the starting SiC powders F (MSC-20), M (A20) and C (A10).

As predicted by the particle size distributions in Fig. 1, the SiC powder F had fine particles with a relatively uniform particle size distribution. Powders M and C were coarser, and for the powder C, most particles were larger than 1 μm and large particles up to 5 μm were observed. The content of the SiC powder in Al_2O_3 was varied from 1 to 10 vol%. In all powder mixtures 0.1 wt% of MgO as Mg-acetate (99% purity, Yacuri Pure Chemicals, Co., Ltd., Japan) was added to nullify the undesirable effect of the SiO_2 impurity mainly from the SiC powder on the sintering behavior [10]

The starting powders were mixed in ethanol first with an ultrasonic probe for 5 min. Then, ball milling was performed for 1 h in a polyurethane jar. Grinding media were zirconia balls of a 6 mm diameter made by Tosoh Corp., Japan and contained 3 mol% Y_2O_3. Drying of the ball-milled slurry was performed in a rotary evaporator using a horizontal glass cylinder as slurry container. The water bath for heating was maintained at 70°C and it took approximately 30 min for complete drying. The dried pieces were very soft and passed a stainless steel screen of 120 US mesh. Pellets of 12.5 mm $\phi \times 4$ mm as well as rectangular bars of $32 \times 32 \times 10$ mm were made in hardened steel dies using a hydraulic press under a pressure of 20 MPa. These pellets or bars were isostatically pressed under a 272 MPa pressure in rubber bags with a wet cold-isostatic press. The green density was approximately 58% of the theoretical. The pressed samples were heated in flowing dry air at 600°C for 10 h to burn out the organics picked up from the mill jar during milling. Pressureless sintering was performed in a graphite resistance furnace (Centorr Co., USA) in a flowing argon atmosphere for 10 min to 4 h at 1700 to 1850°C. Sintered densities were determined by the Archimedes method. Rectangular samples were machined into $3 \times 3 \times 24$ mm bar specimens for the measurement of

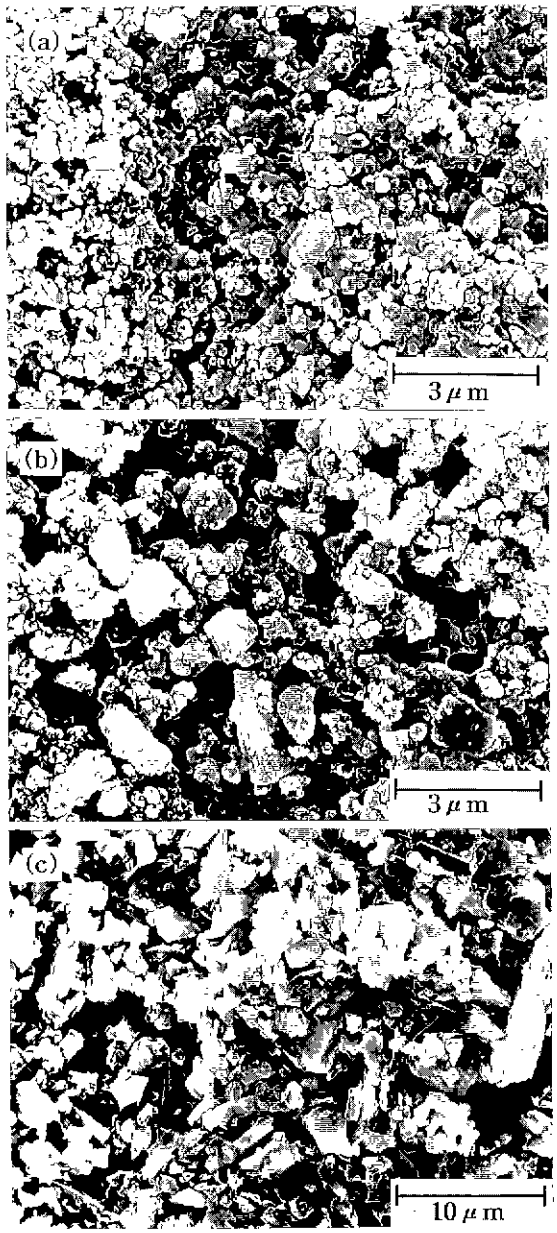

Fig. 2. SEM micrographs of the starting SiC powders (a) F (MSC-20), (b) M (A20) and (c) C (A10).

mechanical properties. Final surface grinding and chamfering of corners were done with 800-grit diamond wheels. Some bar specimens were annealed at 1300°C for 2 h in air.

The 3-point flexural strength was measured with an universal testing machine (AG-500E, Shimadzu Co., Japan), and the span length and crosshead speed were 20 mm and 0.5 mm/min, respectively. Fracture toughness was determined with the SENB (single-edge notched beam) method using a 100 μm-thick diamond wheel to obtain 1.4 mm-deep and approximately 120 μm-wide notches on the specimens. The fracture as well as polished and etched surface of some of the specimens were examined with a scanning electron microscopy (S-4100,

Hitachi Co., Japan) Polishing was done with 6 and 1 μm size diamond pastes. Crack paths were obtained on the polished section by indentation with a Vickers hardness tester (DVK-2S, Matsuzawa Co., Ltd., Japan) under a load of 49 N. Some polished specimens were thermally etched at 1500°C for 10 min in an argon atmosphere and the average grain sizes were determined from the scanning electron micrographs by the linear intercept method with the conversion factor of 1.5.[11]

III. Results and Discussion

1. Sintering behaviors

Fig. 3 shows the relative densities of the sintered specimens containing SiC powders F and M as a function of the SiC content. The specimens were sintered at 1700°C for 4 h. As a reference, pure alumina, using the same starting alumina powder without SiC addition, could be sintered to a density higher than 99% of the theoretical at 1500°C in one hour. In general, the sintered density decreased as the SiC content increased, and the specimens containing the SiC powder F (termed composite F) showed lower densities than those containing the SiC powder M (termed composite M). As expected, the second phase particles retarded densification and this effect was bigger with smaller second phase particles at the same amount. However, the composite M containing 1.0 vol% SiC showed a relatively low density deviating from the expectation. This seems to be caused by rapid and less-uniform grain growth occurred in the sample with 1.0 vol% SiC. The average grain size as a function of the SiC content is presented in Fig. 4. The trend of inhibition of grain growth by SiC particles was similar to the retardation of densification. The effect of the second phase particle size on growth of matrix grains has been well known from Zener's relationship.[6] As predicted, smaller SiC particles inhibited grain growth more severely, and the relatively small change in the mean particle sizes of SiC from 0.28 to 0.44 μm resulted in a significant reduction in the matrix grain sizes of these particulate composites.

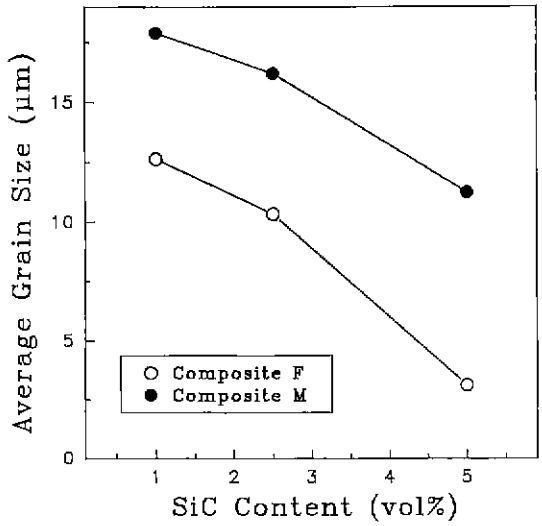

Fig. 4. Average grain size versus SiC content for composites F and M sintered at 1700°C for 4 h.

Relative densities for the composites containing 10 vol% SiC and sintered for 4 h at 1800°C and 1850°C are depicted in Fig. 5 and Fig. 6, respectively. The composite containing the SiC powder C was termed as composite C. As for the density data of the previous specimens sintered at 1700°C, the densification rate of the composite with smaller SiC particles was lower than those of the samples with larger SiC particles. After the composites reached certain densities in less than an hour, they

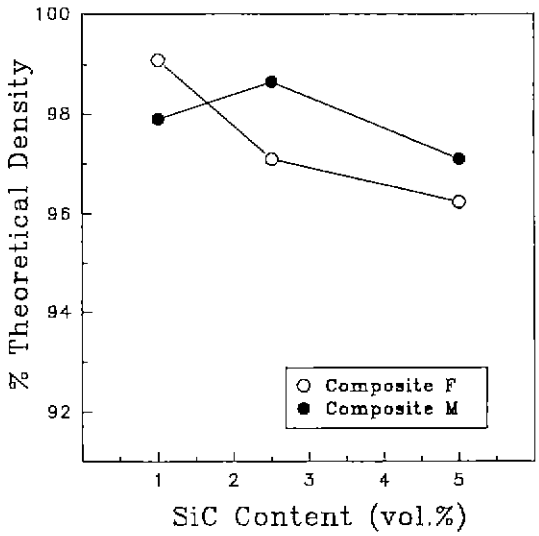

Fig. 3. Relative density as a function of the SiC content for Al_2O_3/SiC particulate composites F and M sintered at 1700°C for 4 h.

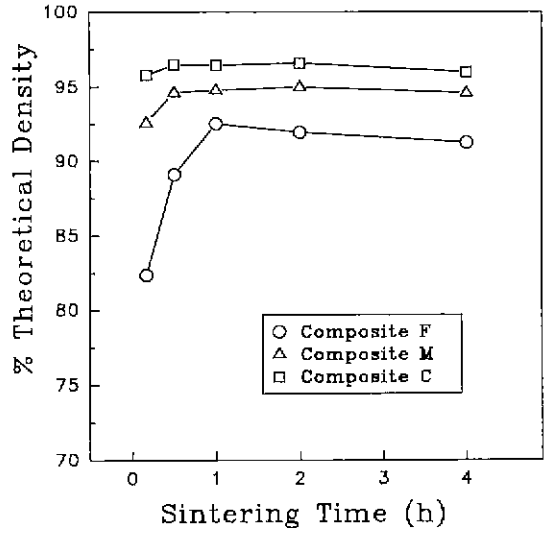

Fig. 5. Relative density as a function of the sintering time for composites F, M and C containing 10 vol% SiC and sintered at 1800°C.

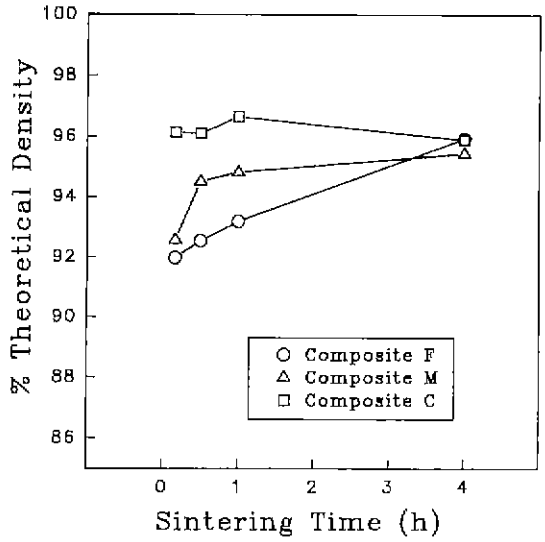

Fig. 6. Relative density as a function of the sintering time for composites F, M and C containing 10 vol% SiC and sintered at 1850°C.

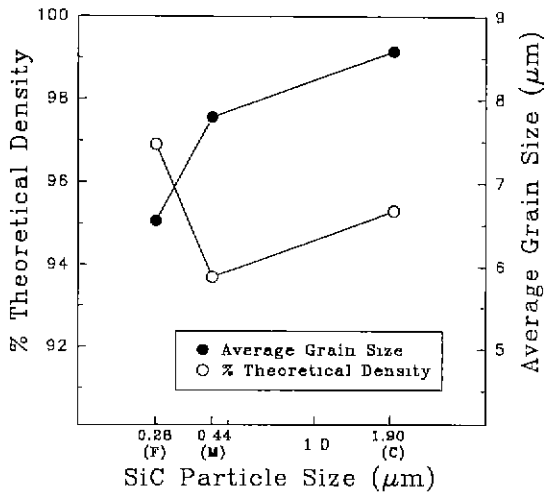

Fig. 7. Average grain size and theoretical density of the composites containing 10 vol% SiC as a function of the median particle size of the starting SiC powder. The composites F (0.28 μm), M (0.44 μm) and C (1.9 μm) were sintered at 1850°C for 4 h and the density data presented here were for the test bars machined from large rectangular specimens.

stopped shrinking especially for the specimens sintered at 1800°C. These limiting densities may be due to the rapid opening of large pores which can not be densified as discussed soon. Only at 1850°C after 4 h, all the composites containing 10 vol% SiC particles obtained densities higher than 95% of the theoretical. It is noted that the composites containing larger particles tended to reach the limiting densities quickly while the composite containing 0.28 μm SiC particles was sintered more slowly but kept on shrinking during the sintering time of 4 h. The resultant density of the composite F after 4 h sintering was eventually higher than those of the composites M and C as shown in Fig. 6. It is believed that at a very high sintering temperature the relative size of pores opened up by the fine inclusion particles was not big enough as compared with the matrix grains to stop the densification.

For the inclusions which do not coalesce as in the case of SiC, a rigid network of touching or near-touching inclusion particles can form to retard densification.[12] Alternatively, different transient stress fields in the radial and hoop directions in the matrix near the inclusions during sintering can lead to local desintering in the compact.[13] Both mechanisms results in opening of large crack-shaped pores. Once large pores as compared with the matrix grain sizes are formed, then they can grow rather than shrink during sintering [14] Therefore, the compact can reach a certain limiting density after some sintering time and does not shrink any more. In this study, at the same SiC content, the densification rate decreased more as smaller SiC particles were added. A similar shrinkage behavior depending on the SiC particle size has been reported for a ZnO-SiC system where the dispersed SiC particles were always larger than the matrix grain size.[15] However, this study and another one with very fine SiC particles having the average particle size of much less than 0.1 μm performed in this lab[16] showed that the densification rate was a strong function of the inert dispersed particle size and as the dispersed particle size was finer, the densification rate was lower regardless of the relative size between the matrix and dispersed particles or of the dispersed particle content. The exact mechanism for the strong dependency of the densification rate on the SiC particle size is not known yet.

The average grain size after sintering 4 h is presented in Fig. 7 and compared with the sintered density. Data for the density as well as grain size shown in this figure were obtained from the test bars made from the large rectangular specimens and, therefore, the density data were somewhat different from those of the small pellets shown in Fig. 6. The average grain size was again smaller with smaller SiC particles as discussed previously for the composites sintered at 1700°C. However, the lower density or higher porosity of the composite should have also contributed to retardation of the matrix grain growth to some extent especially for the composite M. In case of the composite F, the relative porosity to those of composites M and C changed during sintering and, therefore, it was not clear for this specimen how the porosity affected the resultant matrix grain size as compared with those of other composites.

2. Microstructures

Fig. 8 shows SEM micrographs of fracture surfaces of the composites F and C sintered at 1700°C for 4 h. The microstructure of the composite F was relatively uniform in general and the grain size was smaller. As the amount of SiC increased, the microstructure became finer and more uniform. Although it is not clearly shown in

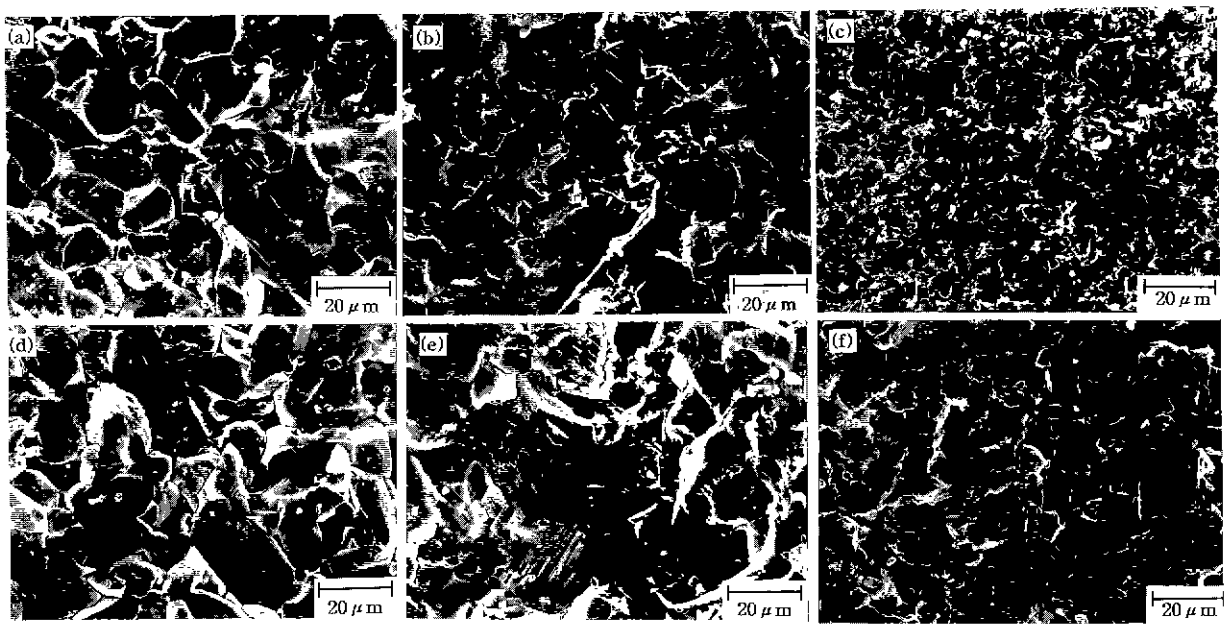

Fig. 8. SEM micrographs of fracture surfaces of the composites F containing (a) 1.0, (b) 2 5 and (c) 5.0 vol% SiC as compared with the composites M containing (d) 1.0, (e) 2.5 and (f) 5.0 vol% SiC. All specimens were sintered at 1700°C for 4 h.

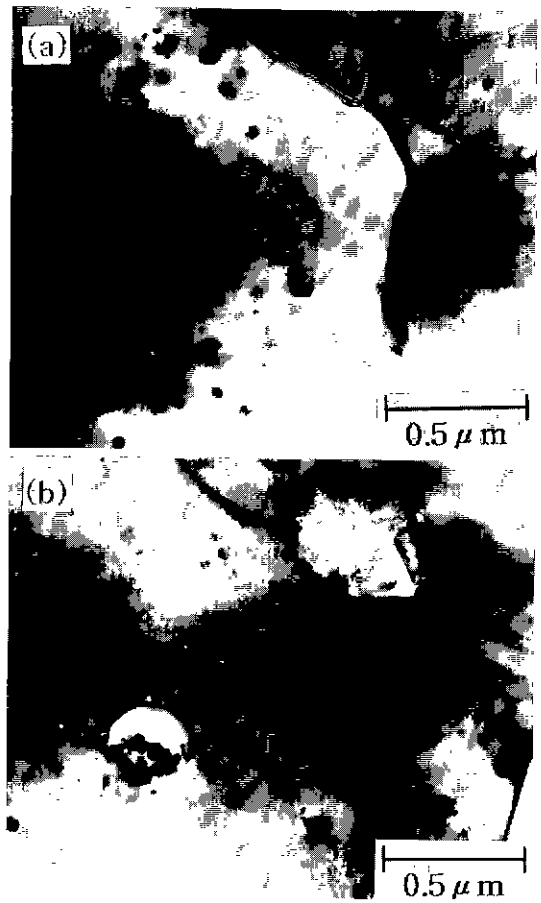

Fig. 9. Typical TEM micrographs of the composites (a) F and (b) M containing 5 vol% SiC and sintered at 1700°C for 4 h.

these pictures, abnormal grain growth was observed occasionally for the composite M containing 1.0 and 2.5 vol% SiC. For these amounts the numbers of SiC particles were insufficient for retarding grain growth uniformly. Fig. 9 shows typical TEM micrographs of the composites F and M containing 5 vol% SiC. In the composite F, fine SiC particles were mainly inside the matrix grains with some on the grain boundary. The number of fine SiC particles inside the grains were much less for the composite M than that for the composite F and large particles were observed on most of the grain boundaries.

Fig. 10 presents the SEM micrographs of fracture surfaces of the composites F, M and C containing 10 vol% SiC and sintered at 1850°C for 4 h. Again, the matrix grain sizes became larger with larger SiC particles. In nanocomposites, intragranular second-phase particles near the grain boundary may exert compressive stresses due to the residual thermal stress resulting in strengthening of the grain boundary while the residual thermal stress around intragranular particles cause matrix weakening.[9] Therefore, nanocomposites tend to show transgranular fracture as depicted in Fig. 10(a) and (b) for composites F and M, respectively. In the composite C, however, SiC particles were relatively large and few particles were entrapped inside the matrix grains, and, as a result, more intergranular fracture was observed as shown in Fig. 10(c). The traces of SiC particles pulled out during fracture as indicated with arrows were observed abundantly especially on the grain boundaries while some SiC particles pointed with triangles were exposed after fracture and still attached to the alumina matrix grains.

3. Mechanical properties

Fig. 11 shows the flexural strength of the composites F

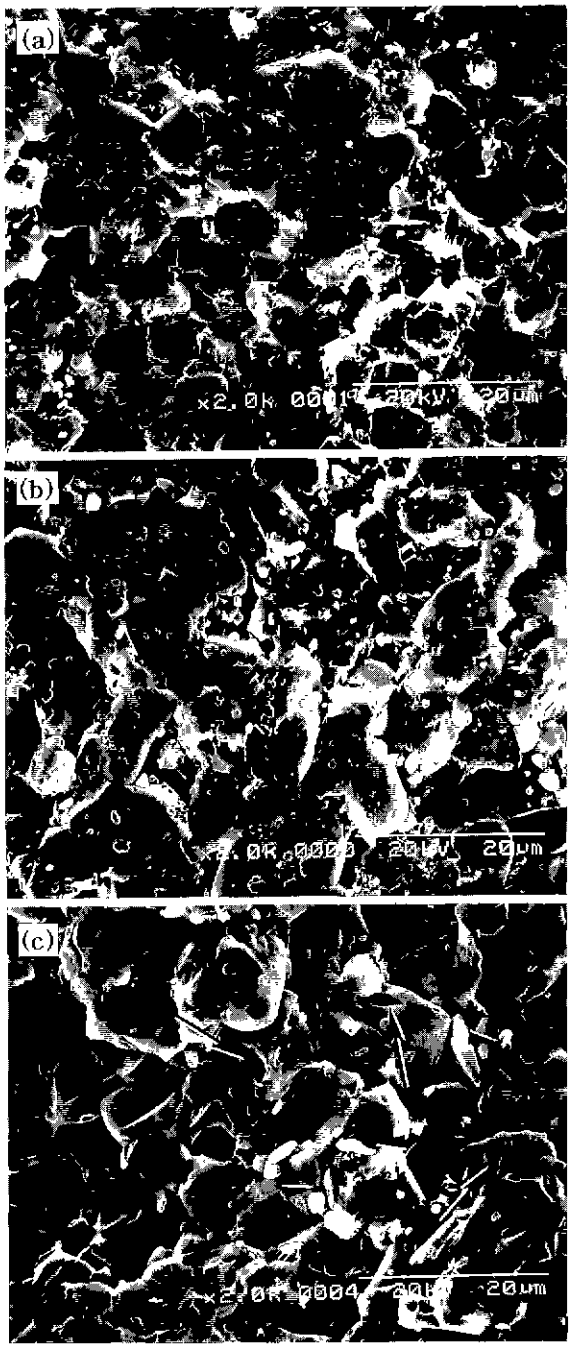

Fig. 10. SEM micrographs of fracture surfaces of the composites (a) F, (b) M and (c) C containing 10 vol% SiC and sintered at 1850°C for 4 h.

and M as a function of the SiC content. The 10 vol% SiC specimens were sintered at 1850°C and the specimens with less SiC were sintered at 1700°C. The flexural strength showed a maximum at 5 vol% SiC. A theoretical analysis[9] predicted that the addition of 5 vol% of fine particles going into the matrix grains would give maximum toughening and thereby strengthening effects of SiC particles and the prediction seemed to be valid in this study. However, it has been well shown in a literature[7] that the flexural strength of the hot-pressed nano-

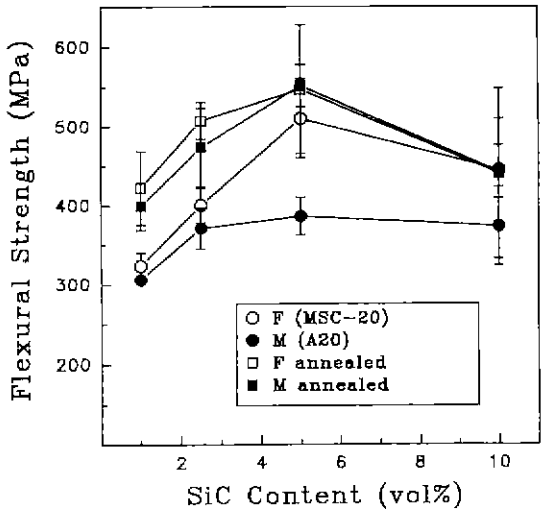

Fig. 11. Flexural strength as a function of the SiC content for composites F and M as sintered at 1700°C (1.0 to 5.0 vol%) or 1850°C (10 vol%) for 4 h as well as after annealing at 1300°C for 2 h.

composite containing 5 vol% SiC of a similar particle size as that of the powder F was approximately same as that of the hot-pressed pure alumina when the grain size was similar each other. Therefore, the lower strength of the current specimens containing less than 5 vol% SiC should not be interpreted as less strengthening due to less SiC particles, and the agreement with the theory could be coincidental. More reasonable explanation for the maximum strength at 5 vol% may be found from elsewhere. As shown previously, the microstructure became finer and more uniform when the amount of SiC increased to 5 vol%. At 10 vol%, the specimens were sintered at a much higher temperature and the grain size was larger. Therefore, the highest strength with 5 vol% SiC particles in this study may be owing to the more uniform microstructure as well as smaller grain size resulting in a smaller critical flaw size. This explanation seems to be even more plausible when the strengths of annealed specimens are compared each other between composites containing different SiC particle sizes. When the machined bar specimens were annealed at 1300°C for 2 h, the strength increased as expected. It has been well known for the nanocomposites that machining flaws are healed during annealing but the compressive surface stress caused by machining does not disappear owing to the SiC particles.[3] After annealing, the strengths of the composites M and F at 5 vol% became approximately same each other. Since the composite F had much more SiC particles inside the grains, the intrinsic strength or the strength without the effect of machining flaws obtained after annealing should be higher than that of the composite M if the higher strength before annealing was due to the strengthening effect of intragranular SiC particles. The same intrinsic strength obtained after annealing regardless of the amount of intragranular SiC

particles implies that the large strength difference before annealing was due to the different machining flaw sizes usually caused by the different grain sizes. Even for 10 vol% specimens, the intrinsic strengths obtained after annealing were same each other between the composites F and M. Therefore, the fine SiC particles inside Al_2O_3 grains might not be truly effective to improve the intrinsic strength of Al_2O_3. The lower strength of the composite F containing 10 vol% SiC than that of the composite F containing 5 vol% SiC could be caused by the approximately twice larger gain sizes of the 10 vol% composite due to the higher sintering temperature. Finally, it is notable that the strength improved considerably after annealing even when the amount of added SiC particles was as small as 1.0 vol% for both mean SiC particle sizes of 0.28 and 0.44 μm.

Fracture toughness of the composites F and M is presented in Fig. 12 as a function of the SiC content. For both composites the toughness change according to the increase of the SiC content was small. The addition of 0.28 μm SiC particles in Al_2O_3 up to 5 vol% did not improve fracture toughness appreciably, although fracture toughness fluctuated somewhat, similar to the data obtained for hot-pressed dense composites reported in the literature [7] For the composite M, fracture toughness decreased gradually to some extent as more SiC was added, but, in any case, it is difficult to understand the reason for the slight toughness change as a function of the SiC content considering the different microstructures and porosity of the samples.

In Fig. 13 the flexural strength and fracture toughness of the composites F, M and C containing 10 vol% SiC are compared among each other. The strength of the composite M was the lowest, which might reflect the relatively low density of the specimen as shown earlier in Fig. 6. However, the annealed strengths were same each other among the three different composites as in the

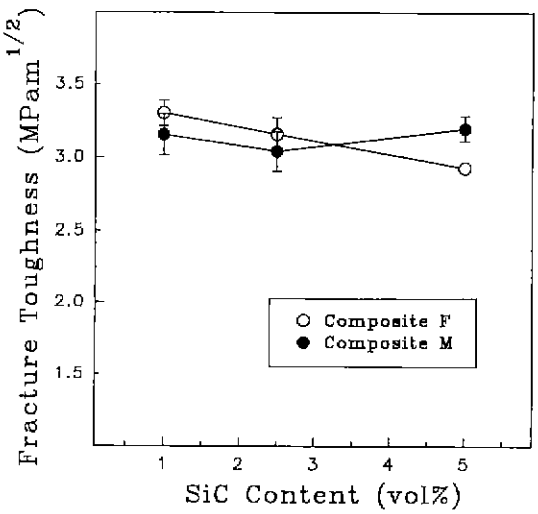

Fig. 12. Fracture toughness as a function of the SiC content for the composites F and M sintered at 1700°C for 4 h

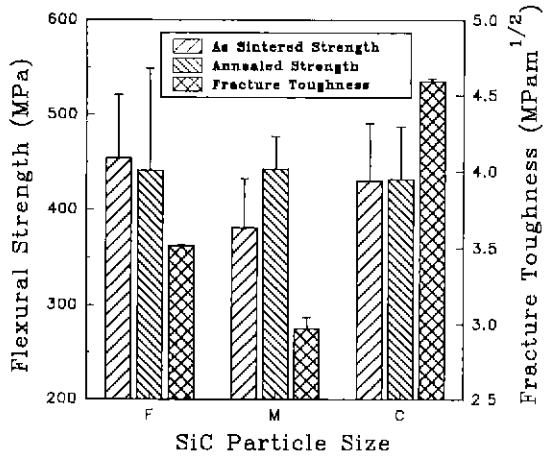

Fig. 13. Flexural strength, as-sintered and after annealing, and fracture toughness of the composites F, M, and C containing 10 vol% SiC and sintered at 1850°C for 4 h

case of 5 vol% SiC samples discussed earlier. This again implies that fine SiC particles inside Al_2O_3 grains were not effective to improve the intrinsic strength. On the other hand, fracture toughness of the composite C was 4.6 MPa, which was 30 to 50% higher than those of others. Remembering the intergranular fracture and pull-out of SiC particles of this relatively tough composite as previously shown in Fig. 10(c), crack deflection and crack bridging by the SiC particles might be considered as toughening mechanisms. Fig. 14 presents the crack paths for the composites obtained by indentation on the polished sections. For the composite F, the crack path shown in Fig. 14(a) was straight in general due to the transgranular fracture while the crack shown in Fig. 14(c) for the composite C seemed to follow the grain boundary. The crack on the composite M often found pores due to the high porosity. For the composite C, crack deflection around SiC particles and crack bridging by SiC particles were observed frequently and are well shown in Fig. 14(c) as pointed with arrows. In addition, matrix grain bridging, as indicated with a triangle in Fig. 14(d) together with bridging by a SiC particle, is observed occasionally. Therefore, crack bridging by the alumina matrix grains found in normal monolithic alumina ceramics[17] also contributed to the toughening improvement to some extent for this composite owing to more intergranular fracture. Crack bridging was also observed even in the composite F but much less frequently and in smaller scales as shown in Fig. 14(a). Aggregates of fine SiC particles seemed to be the bridging particles in the composite F containing 10 vol% SiC of 0.28 μm particles. Crack bridging by SiC particles should have also occurred to some extent in the composite M, however, it did not seem to be enough to compensate completely the negative effect of the high porosity as shown in Fig. 14(b), and fracture toughness of the composite M was relatively low as a result. Since the grain bridging effect is stronger with larger grains,[18] crack bridging

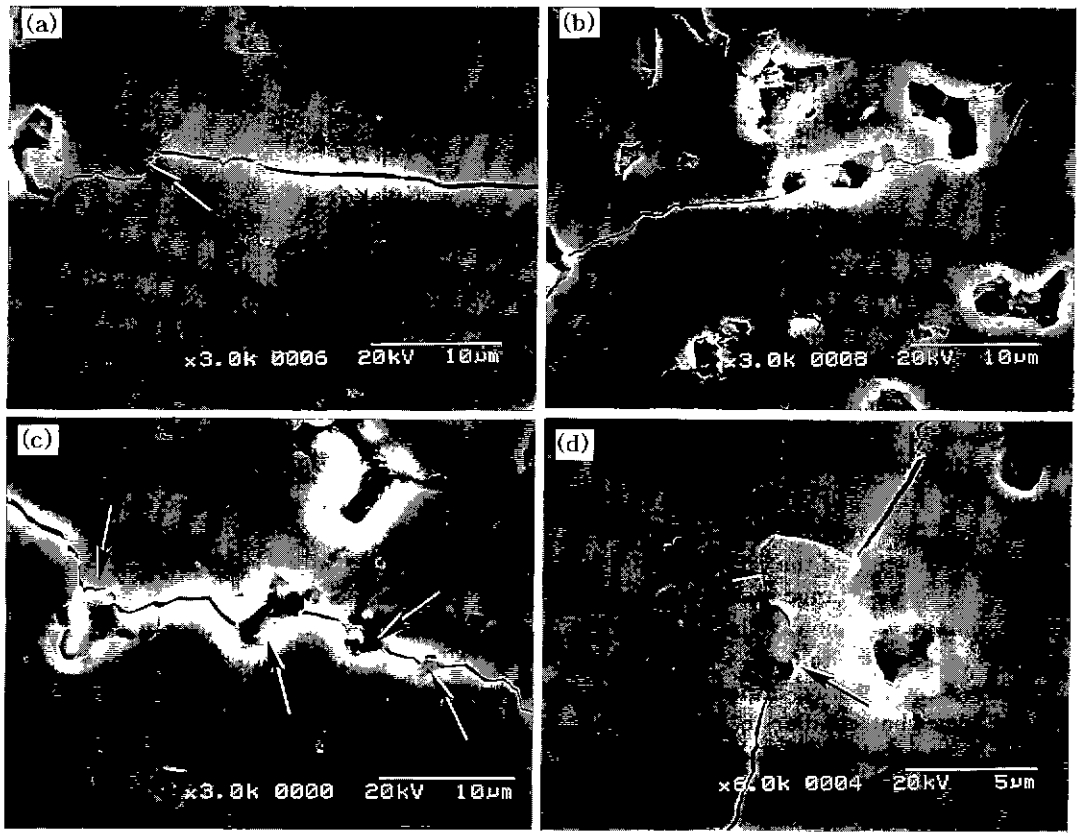

Fig. 14. Crack paths obtained by indentation of composites (a) F, (b) M and (c. d) C containing 10 vol% SiC and sintered at 1850°C for 4 h. Arrows in (a), (c) and (d) indicate crack bridging by SiC particles while the triangle in (d), by an alumina matrix grain.

should be more effective in the composite C containing 1.9 μm SiC than in others containing smaller SiC particles. In a similar system of the SiC platelet/alumina composites, crack deflection had been reported as the main toughening mechanism.[19] The specimens had large SiC platelets with a mean size of 24 μm and the alumina grains were much finer than the platelets. However, in the current specimens containing relatively small SiC particles in large alumina matrix grains, it is believed that crack bridging by SiC particles was the main toughening mechanism for the composite C containing 1.9 μm SiC. On the other hand, grain bridging by alumina matrix grains also contributed to the toughening to some extent, and, furthermore, crack deflection by SiC particles can not be ruled out completely as an additive toughening mechanism.

IV. Conclusions

Al_2O_3/SiC particulate composites were fabricated by pressureless sintering at either 1700°C or 1850°C depending on the SiC content. The SiC content in the composites was varied from 1.0 to 10 vol% and three different SiC powders having different medium particle sizes from 0.28 μm to 1.9 μm were used. Both densification and grain growth were retarded more as the SiC particles were smaller. The microstructure of the composite was finer and more uniform with higher SiC content except the 10 vol% specimens, which were sintered at a higher temperature. The maximum flexural strength was obtained with 5 vol% SiC regardless of the SiC particle size owing to the more uniform and finer microstructures of the composite. Annealing of the composites at 1300°C for 2 h improved the strength in general and this annealing effect was good even for the specimens with as low as 1.0 vol% of SiC. The toughness did not increase appreciably as the SiC content increased up to 5 vol%. However, for the 10 vol% SiC composites, markedly higher fracture toughness was obtained with the specimen containing 1.9 μm SiC particles. It was found that relatively large SiC particles stayed on the grain boundary causing intergranular fracture and induced crack bridging to improve the toughness of this specimen.

Acknowledgement

This research was supported by the Yeungnam University Research Grant in 1996.

References

1. K. Niihara, "New Design Concept of Structural Ceramics

– Ceramic Nanocomposite." *J. Ceram. Soc. of Jpn. Int Edition*, **99**[10], 945-52 (1991).
2. K Niihara, K. Izaki and T. Kawakami, "Hot-Pressed Si_3N_4-32% SiC Nanocomposite from Amorphous Si-C-N Powder with Improved Strength above 1200°C," *J. Mat. Sci. Letter*, **10**, 112-14 (1990).
3. A. M. Thompson, H. M Chan and M. P. Harmer, "Crack Healing and Stress Relaxation in Al_2O_3-SiC "Nanocomposites"," *J. Am. Ceram Soc.*, **78**[3], 567-71 (1995).
4. T. Ohji, T. Hirano, A. Nakahira and K. Niihara, "Particle/Matrix Interface and Its Role in Creep Inhibition in Alumina/Silicon Carbide Nanocomposites," *J. Am. Ceram. Soc* , **79**[1], 33-45 (1996).
5. T. Ohji, A. Nakahira, T. Hirano and K. Niihara, "Tensile Creep Behavior of Alumina/Silicon Carbide Nanocomposites," *J. Am. Ceram. Soc.*, **77**[12], 3259-62 (1994).
6. L. C. Sterns and M. P. Harmer, "Particle-Inhibited Grain Growth in Al_2O_3-SiC: II, Equilibrium and Kinetic Analyses," *J. Am. Ceram. Soc.*, **79**[12], 3020-28 (1996).
7. J. Zhao, L. C. Stearns, M P. Harmer, H. M. Chan and G. A. Miller, "Mechanical Behavior of Alumina-Silicon Carbide Nanocomposites," *J. Am. Ceram. Soc.*, **76**[2], 503-10 (1994)
8. G. Pezzotti and M. Sakai, "Effect of a Silicon Carbide Nano-Dispersion on the Mechanical Properties of Silicon Nitride," *J. Am. Ceram. Soc.*, **77**[11], 3039-41 (1994).
9. I. Levin, W. D Kaplan and D. G. Brandon, "Effect of SiC Submicrometer Particle Size and Content on Fracture Toughness of Alumina-SiC Nanocomposites," *J. Am. Ceram. Soc.*, **78**[1], 254-56 (1995).
10. S. I. Bae and S. Baik, "Critical Concentration of MgO for the Prevention of Abnormal Grain Growth in Alumina," *J. Am. Ceram. Soc.*, **77**[10], 2499-504 (1994).
11. R. L Fullman, "Measurement of Particle Sizes in Opaque Bodies," *J. Metals Trans. AIME*, **197**, 447-52 (1953).
12. F. F. Lange, "Constrained Network Model for Predicting Densification Behaviour of Composite Powders," *J. Mater. Res.*, **2**[1], 59-65 (1987).
13. R K. Bordia and G. W. Scherer, "Overview No. 70 – On Constrained Sintering – Part III. Rigid Inclusions," *Acta Metall.*, **36**[9], 2411-16 (1988).
14. W. D. Kingery and B. Francois, "The Sintering of Crystalline Oxides, I. Interactions Between Grain Boundaries and Pores," pp. 471-96, in Sintering and Related Phenomena, Ed. by G. C. Kuczynski, N. Hooten and C. Gibson, Gordon & Breach Science Publishers, New York, 1967.
15. M. W. Weiser and L. C. De Jonghe, "Inclusion Size and Sintering of Composite Powders," *J. Am. Ceram. Soc.*, **71**[3], C-125-C-127 (1988).
16. J. Ryu and J. Lee, Unpublished data.
17. P. L. Swanson, C. J. Fairbanks, B. R. Lawn, Y – W Mai and B. J. Hockey, "Crack-Interface Grain Bridging as a Fracture Resistance Mechanism in Ceramics: I, Experimental Study on Alumina," *J. Am. Ceram. Soc.*, **70**[4], 279-89 (1987).
18. B. Lawn, Fracture of Brittle Solids-Second Edition, pp. 230-241, Cambridge Univ. Press, Cambridge, 1993.
19. Y. Chou and D. J. Green, "Silicon Carbide Platelet/Alumina Composites: III, Toughening Mechanisms," *J. Am. Ceram. Soc.*, **76**[8], 1985-92 (1993).